ISTITUTO NAZIONALE DI FISICA NUCLEARE - ISTITUTO NAZIONALE DI FISICA NUCLEARE - ISTITUTO NAZIONALE DI FISICA NUCLEARE - ISTITUTO NAZIONALE DI FISICA NUCLEARE - ISTITUTO NAZIONALE DI FISICA NUCLEARE - ISTITUTO NAZIONALE DI

Laboratori Nazionali di Frascati

LNF-90/019(R)
26 Marzo 1990

V. Lucherini, N. Bianchi, E. De Sanctis, C. Guaraldo, P. Levi Sandri, V. Muccifora, E. Polli, A.R. Reolon, P. Rossi, S. Aiello, E. De Filippo, G. Lanzanò, S. Lo Nigro, C. Milone, A. Pagano, A.S. Botvina, A.S. Iljinov, M.V. Mebel:

PROPOSAL OF MEASURING THE MECHANISMS OF NUCLEAR EXCITATION LEADING TO FISSION WITH THE ADONE JET-TARGET TAGGED PHOTON BEAM

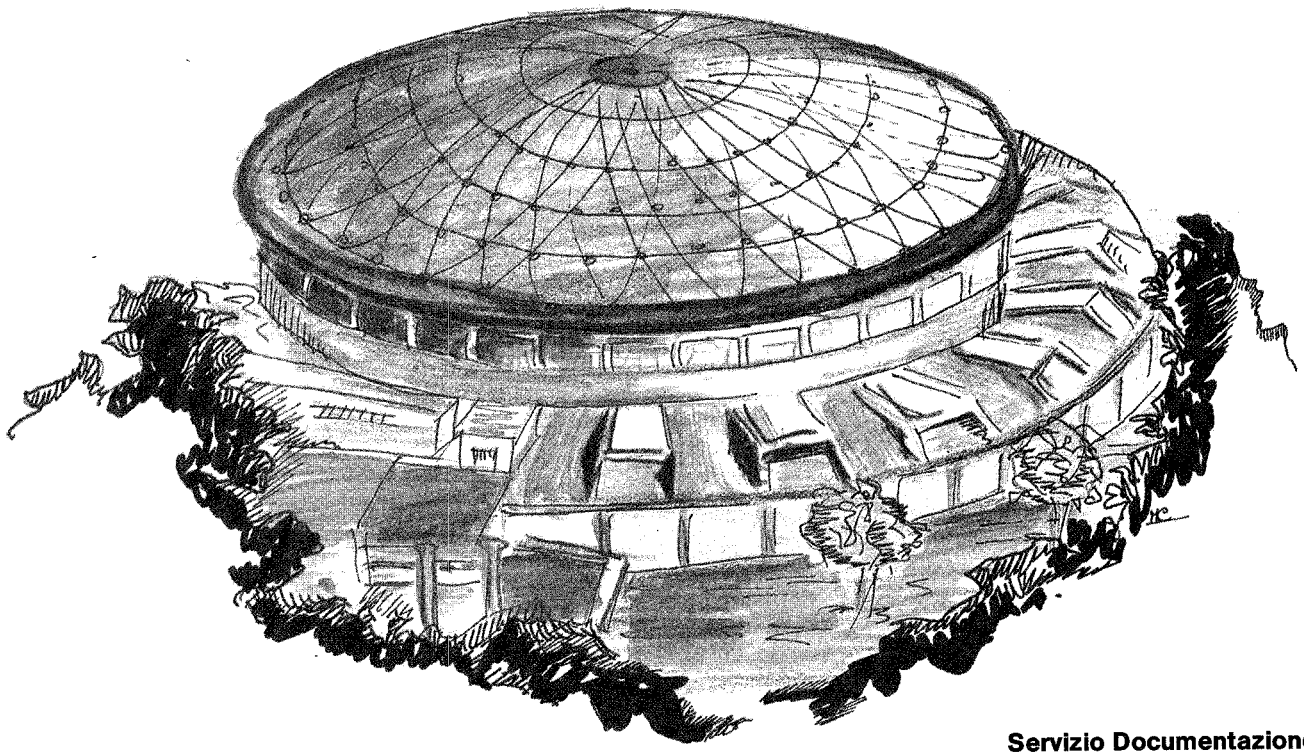

Servizio Documentazione
dei Laboratori Nazionali di Frascati
P.O. Box, 13 - 00044 Frascati (Italy)

INFN - Laboratori Nazionali di Frascati
Servizio Documentazione

LNF-90/019(R)
26 Marzo 1990

PROPOSAL OF MEASURING THE MECHANISMS OF NUCLEAR EXCITATION LEADING TO FISSION WITH THE ADONE JET-TARGET TAGGED PHOTON BEAM.

V. Lucherini, N. Bianchi, E. De Sanctis, C. Guaraldo, P. Levi Sandri, V. Muccifora, E. Polli and A.R. Reolon
INFN - Laboratori Nazionali di Frascati, I-00044 Frascati

P. Rossi
INFN - Sezione Sanità, Roma

S. Aiello, E. De Filippo, G. Lanzanò, S. Lo Nigro, C. Milone and A. Pagano.
INFN - Sezione di Catania e Dipartimento di Fisica dell'Università, Catania

A.S. Botvina, A.S. Iljinov and M.V. Mebel
Institut for Nuclear Research of the Academy of Sciences of USSR, Moscow

ABSTRACT

The mechanisms of excitation with subsequent fission of heavy nuclei can be conveniently studied by means of photons, since this probe is able to interact deeply inside the nucleus. We propose the use of the (200÷1200 MeV) tagged photon beam from the ADONE Jet Target in order to study the mass-energy and total momentum distributions of fission fragments, to obtain experimental information on the configurations (excitation energy and nucleonic composition) of produced compound nuclei and on their decay channels.

1. INTRODUCTION

Fission is an interesting channel to study the collective modes of excitation of nuclei for three clear-cut reasons:

1) it is a genuine collective phenomenon, since all nucleons in the nucleus are involved;
2) it is a "slow" process ($t > 10^{-21}$s) with respect to nuclear scale times ($t < 10^{-22}$s), hence allowing the study of nuclei in thermodynamic (equilibrium) states far from the ground state;
3) it is present also at intermediate-high energies (>200÷300 MeV), thus giving the opportunity of pumping enough energy into a nucleus to see the appearance of possible unusual phenomena. In fact, if one deposits some hundred MeV inside a heavy nucleus, with small angular momentum, one can study in a clean way nuclear thermal effects, in particular the excitation energy dependence of the fission barrier.[1] Eventually, one could approach an energy density where nuclear phase changes are anticipated.[2]

Moreover, in heavy nuclei, fission reactions give information on the absorption process of the probe because, as in the case of photonuclear[3] or pion absorption,[4] a large part of the reaction cross section is due to nuclear fission. Finally, delayed fission allows to study the Λ-hypernuclei production initiated by the interaction of an electromagnetic (electron)[5] or hadronic (antiproton)[6] probe.

To these facts, one must also add the relative simplicity, from an experimental point of view, in identifying a fission reaction through the very large pulses of the strongly ionizing fission fragments.

For these reasons, in recent years there has been a renewed attention in fission induced in heavy nuclei by intermediate-high energy probes, as protons[7] and monochromatic photons,[8] or by probes able of releasing high excitation inside nuclei, as pions[4] and, more recently, antiprotons.[9] In a recent paper,[10] we showed that, in deep inelastic interactions of intermediate energy particles with heavy nuclei, it is formed a thermalized highly excited system (*residual nucleus*) of universal nature, which decays in fission products independently of the method of formation. This was shown by studying fissility of Au, Bi and U nuclei by intermediate energy monochromatic photons (k=200 MeV), protons (E_p=190 MeV) and pions (E_π=80 MeV), whose primary energies where selected in order to produce residual nuclei of similar average excitation energy ($\langle E^* \rangle \approx 75$ MeV), angular momentum spectra and Z and A composition.

In pursuing this study at higher excitation energies ($E^* \geq 100$ MeV), one is faced with a main problem: it is more and more difficult in reactions initiated by different probes to find residual nuclei which show similar distributions of their configurations. In fact, at incident energies above ≈200 MeV, the excitation energy distributions of residual nuclei become increasingly flat and wide (as it is seen in Fig. 1, for the photon case), so that the measured fission quantities are the result of a smearing over these wide distributions, and it is hard to extract the actual dependence of the process on each variable.[11]

Accurate photofission data at high nuclear excitation could be used in comparison with results on fission obtained with other probes that transfer low angular momentum to the struck

nucleus, and also with data obtained with heavy ion to isolate angular momentum effects. With the recent advent of monochromatic photon beams with energy up to the GeV region[12] and of intense low energy antiproton beams,[13] it is now opened the possibility of studying experimentally this domain. On the theoretical side, the sophisticated Intranuclear Cascade (INC) Monte Carlo models allow to describe with reliable accuracy the development of the cascade due to the absorption of the energetic probe and the subsequent deexcitation by evaporation-fission processes.[1,14]

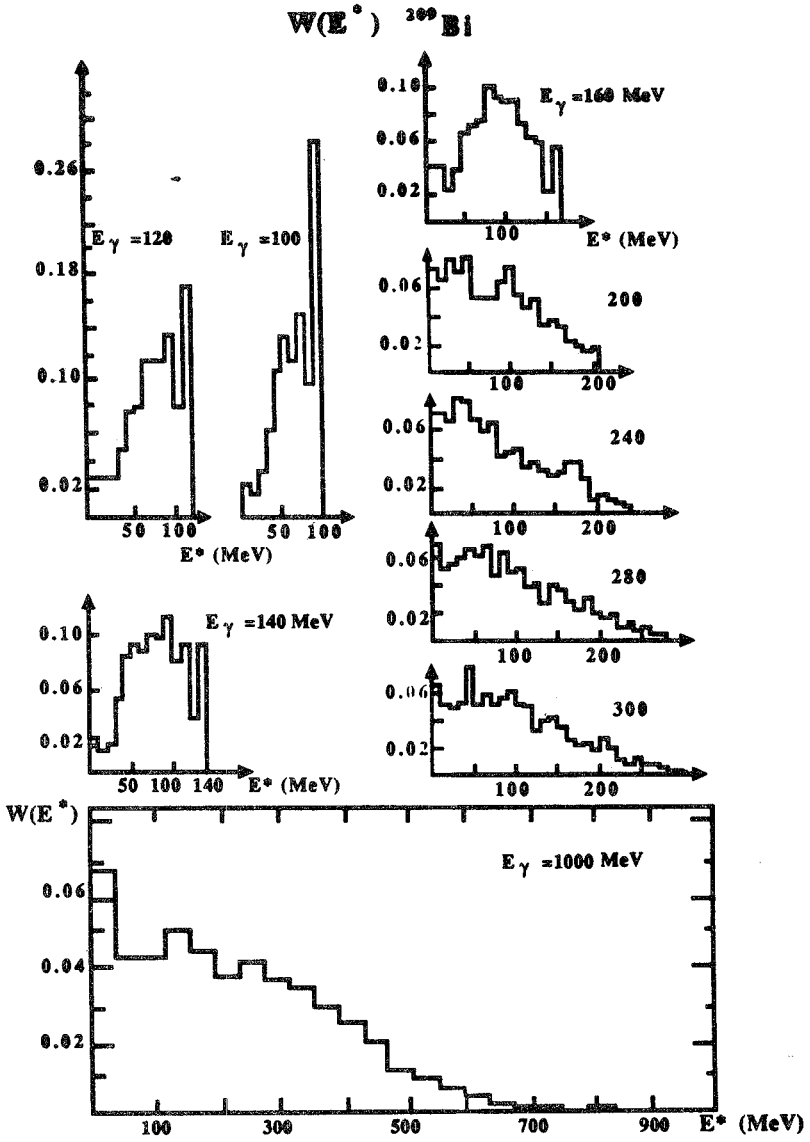

FIG.1 - Excitation energy distributions W(E*) of compound nuclei formed in the interaction of monochromatic photons of different energies with ^{209}Bi nuclei, calculated by means of an intranuclear-cascade Monte Carlo code.

The use of photons in the study of fission of highly excited nuclei is advantageous, since photons are very effective, due to their volume absorption, in heating the nucleus, transferring, at same time, relatively low angular momentum to the struck nucleus, contrarily to heavy ion

reactions (high angular momentum effects are very important in fission but complicated to take into account). However, to really identify the specific excitation states of residual nuclei produced by "high exciting" probes, it is necessary to accurately measure not only integral quantity, as total fission cross section, but a more complete set of physical data must be collected. In particular, the characteristics of both fission fragments contain rich information about the excited nucleus: the mass A and charge Z of the fragments allow to reconstruct the mass A_{cn} and charge Z_{cn} of the compound nucleus, and the angle between fragments and their energy the total momentum of compound nucleus before fission.

Fission is a very complicated process: using the above mentioned INC codes, one can try to study which quantities should be measured, with a "minimal" experimental effort, in order to gain the maximum of information on fission at high excitation energy.

In this respect, interesting possibilities are offered by the measurement of mass-energy-momentum distributions of fission fragments with monochromatic photons, to investigate the excitation energy dependence of mass distributions comparing the data taken at different photon energy k. Moreover, when the incoming photon energy is sufficiently high (≥ 1GeV), so that the excitation energy of residual nuclei is comparable with its total binding energy, a different decay channel may open for the hot nucleus, specifically multifragmentation, a phenomenon which could mark the transition of nuclear matter to a new phase,[2] and for which a Monte Carlo model was recently developed.[15]

In this paper we describe the physical motivations and the experimental apparatus designed to measure the relevant quantities from fission of heavy nuclei induced by the (200÷1200 MeV) tagged photon beam from the ADONE Jet Target.

2. NUCLEAR EXCITATION LEADING TO FISSION

2.1 Mass-Energy distributions of fission fragments

The traditional theory of mass distributions of fission fragments is based on the framework of the statistical model of fission (see P. Fong, Ref.16). According to this picture, when a nucleus with mass A, charge Z and excitation energy E* disintegrates by fission in two fragments of masses A_1 and A_2=A-A_1, and most probables charges Z_{P_1} and Z_{P_2}=Z-Z_{P_1}, it is possible to write the following expression for the mass-charge distributions $W(A_1,A_2,Z_{P_1},Z_{P_2})$ of the two fission fragments:

$$W(A_1,A_2,Z_{P_1},Z_{P_2}) \approx \frac{(a_1a_2)^{\frac{1}{2}}}{(a_1+a_2)^{\frac{13}{4}}} \left(\frac{A_1^{\frac{5}{3}} A_2^{\frac{5}{3}}}{A_1^{\frac{5}{3}}+A_2^{\frac{5}{3}}} \right)^{\frac{3}{2}} \left(\frac{A_1A_2}{A_1+A_2} \right)^{\frac{3}{2}} \frac{(Z_{P_1}Z_{P_2})^{\frac{1}{2}}}{\left(B_{A_1}+B_{A_2}-C_{12}\right)^{\frac{1}{2}}} G^{\frac{11}{4}}.$$

$$\cdot\, exp\left[2\sqrt{(a_1+a_2)\,G}\right]\left[1-\frac{19}{4}\frac{1}{\sqrt{(a_1+a_2)\,G}}\right], \tag{1}$$

where a_1 and a_2 are the level density parameters of the two fission fragments, B_{A_1} and B_{A_2} are parameters in the mass formula,[17] C_{12} is a constant in the expression for the Coulomb energy. G, the total excitation energy at the moment of scission without the potential energy of the two fragments, is given by:

$$G = M^*(A, Z) - M(A_1, Z_{P_1}) - M(A_2, Z_{P_2}) - C - D, \tag{2}$$

where:
$M^*(A, Z) = E^* + M(A, Z)$ is the mass of the fissioning nucleus with excitation energy E*; $M(A_1, Z_{P_1})$, $M(A_2, Z_{P_2})$ are the masses of the two fragments (assumed not excited); $C(Z_{P_1}, Z_{P_2})$ is Coulomb energy at the moment of scission; $D=D_1+D_2$ is the scission deformation energy of the two fragments.

The maximum of the distribution (1) corresponds to the maximum of the function G. At high excitation energies, as those involved with the tagged Adone Jet Target photon beam, shell effects disappear, and we expect symmetric fission: $A_1=A_2=A_{cn}/2$ and $Z_1=Z_2=Z_{cn}/2$, where the suffix *cn* indicates the formed compound nucleus. Hence, the shape of the mass distribution (1) can be obtained expanding in power the function G around its maximum G_0, corresponding to exactly symmetric fission, using the variables $\Delta A=A_i - \overline{A}$, with $\overline{A}=A_{cn}/2$.

The final result obtained for the mass distribution is:

$$W(\Delta A) \approx \exp\left\{-\Sigma\, \Delta A^2\right\} \tag{3}$$

where

$$\Sigma = \left[\left[\frac{11}{8G_0} + \sqrt{\frac{a_{cn}}{4G_0}}\right]\alpha + \frac{20}{A_{cn}^2} + \frac{\omega^2}{2Z_p^2(\overline{A})} + \frac{\rho}{B_A(\overline{A}) - \frac{C_{12}}{2}}\right], \tag{4}$$

with: $a_{cn} = a_1+a_2$, and α, and ρ are coefficients that depend on A_{cn} and on the coefficients of the power expansion and of the used mass formula.

The predicted distribution is gaussian, with $FWHM=2.34/\sqrt{2\Sigma}$. In Fig. 2, it is shown the calculated behavior of this FWHM for ^{238}U (Fig. 2a) and ^{209}Bi (Fig. 2b) as a function of the excitation energy E*.

As it is seen, when the excitation energy increases (i) the fragment-mass distribution becomes symmetric (gaussian), and (ii) its width increases. The result (i) was already known in literature but badly studied with bremsstrahlung photon beams for actinide nuclei because of the predominant asymmetric mass distribution from the Giant Dipole Resonance region. The point (ii) can be used to gain a direct information on the actual excitation state of the residual nucleus.

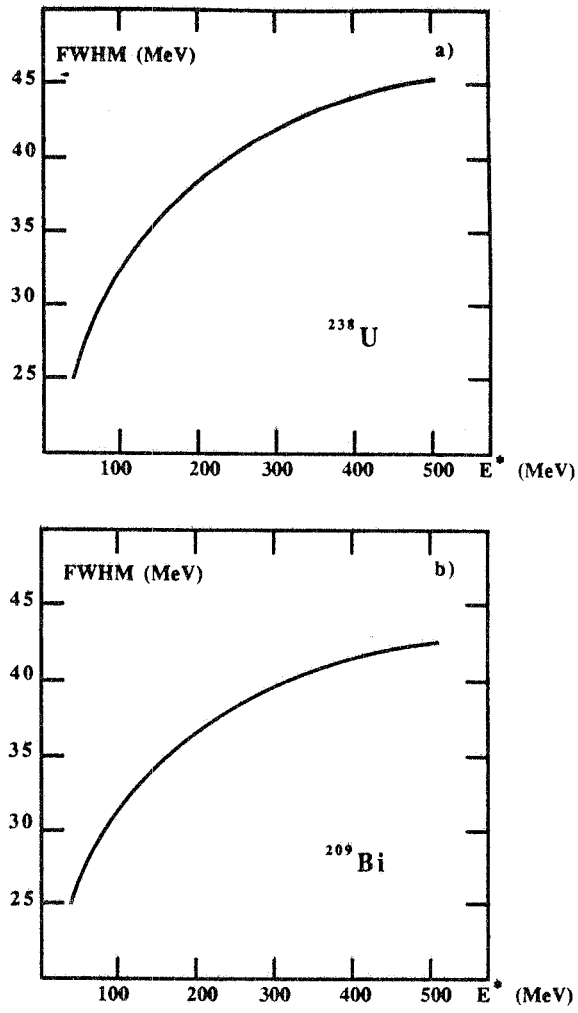

FIG.2 - The FWHM of the mass distribution of fission fragments calculated, in the framework of the statistical model of fission, as a function of the excitation energy E* for: a) ^{238}U; b) ^{209}Bi.

2.2 Total momentum distributions of fission fragments

When the residual nucleus decays through fission, the two fission fragments acquire momenta $\mathbf{P}_1$ and $\mathbf{P}_2$, respectively, while all other light particles emitted at the moment of fission have relatively low momenta. The experimental determination of the excitation energy relative to each fission event is a formidable task from an experimental point of view, because, in principle, it requires an *exclusive* experiment, in which charged and neutral (gammas and neutrons) particles or fragments must be detected. With the use of the INC of Ref.14, however, it is possible to show that the total momentum of the fission fragments $|\mathbf{P}| = |\mathbf{P}_1+\mathbf{P}_2|$ is correlated to the excitation energy of the compound nucleus.

This can be seen in Fig. 3, where the calculated distributions of the residual nucleus excitation energy E* are shown for different values of the total momentum $|\mathbf{P}|$ of the fission fragments, in the case of ^{197}Au photofission with monochromatic photons of energy from 300 MeV up to 1100 MeV. As can be seen, the distribution becomes symmetric and centered at higher excitation energies, as the selected momentum becomes higher. This result is more clearly shown in Fig. 4, where the "center of mass" of the above distributions of E* are shown as a function of $|\mathbf{P}|$.

As a conclusion the elusive and crucial E* quantity of compound nuclei can be determined through the knowledge of $|\mathbf{P}|$. This informations, along with the measurement of the mass and energy distributions of fission fragments, and of the total fission cross section (the fragments angular distribution is nearly isotropic) will give sufficient insight on the actual state of the residual nucleus to put on more quantitative basis the study of fission and of nuclear properties at high excitation energies.

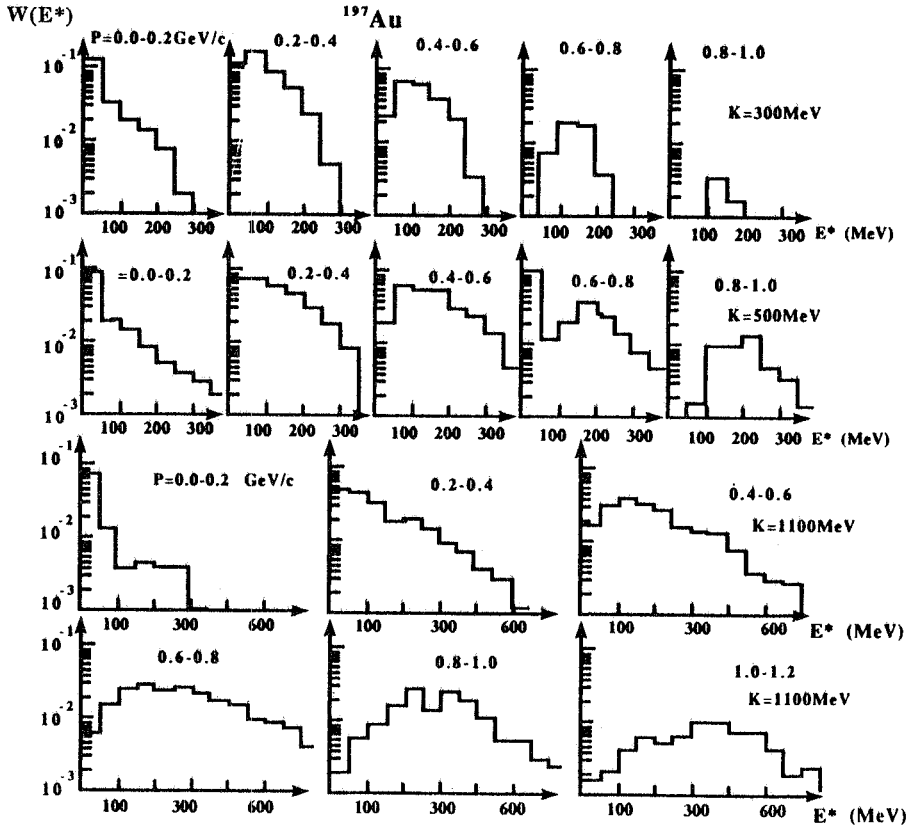

FIG.3 - The excitation energy distribution W(E*) of compound nuclei calculated, by means of an intranuclear-cascade Monte Carlo code, at the given photon energies for selected bins of its total momentum **P**. The calculations are for ^{197}Au nuclei.

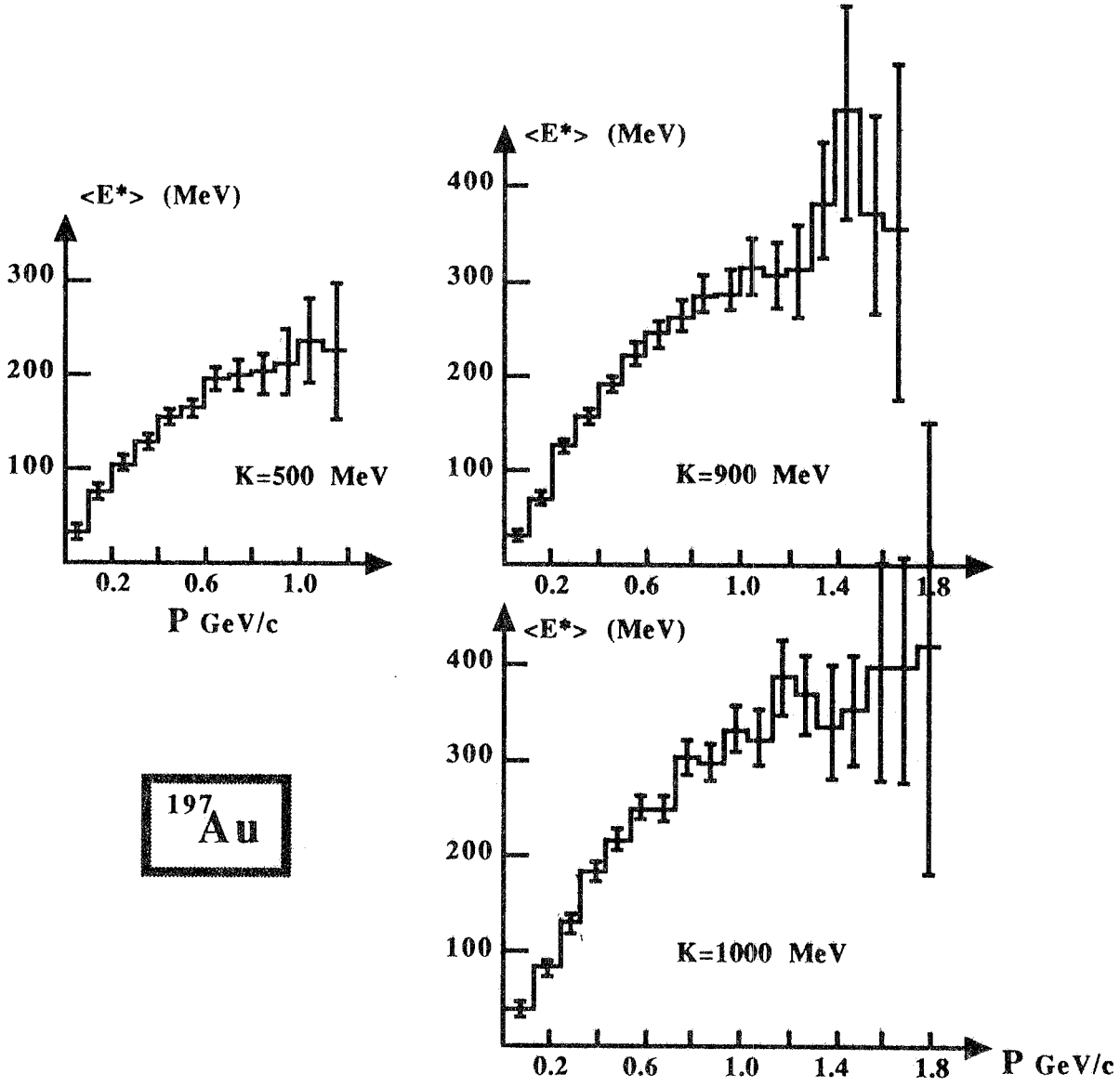

FIG.4 The calculated mean excitation energy <E*> of compound nuclei formed after the interaction of monochromatic photons of selected energies with ^{197}Au nuclei, as a function of its total momentum P.

As a conclusion the elusive and crucial E* quantity of compound nuclei can be determined through the knowledge of $|\mathbf{P}|$. This informations, along with the measurement of the mass and energy distributions of fission fragments, and of the total fission cross section (the fragments angular distribution is nearly isotropic) will give sufficient insight on the actual state of the residual nucleus to put on more quantitative basis the study of fission and of nuclear properties at high excitation energies.

3. NUCLEAR EXCITATION LEADING TO MULTIFRAGMENTATION

When the excitation of the nucleus is close to its total binding energy (E*≥5 MeV/nucleon), a phase transition of the liquid-gas type can occur. Its specific signal is the multiple production of nuclear fragments (of the order of C or O) resulting from the explosive decay of the residual nucleus, a feature referred to as multifragmentation. Needless to stress the conceptual significance of this phenomenon: it is important to understand how a nucleus loses its cohesion as to understand the origin of its self-boundeness. The properties of this phase transition should bear some relationship with the saturating properties of nuclear forces and the nuclear surface tension.

Information about multifragmentation can be obtained from the experiment PS 186 at LEAR[18] (CERN), which used antiprotons. Unfortunately, the experimental method of induced radioactivity applied in that experiment was not sufficiently sensitive or applicable in the mass region where multifragmentation takes place with the used targets. Therefore, no experimental evidence is up to now available about this relevant physical process induced by antiprotons. In Fig. 5, taken from Ref.14, are shown the theoretical predictions for the mass distributions with and without multifragmentation, calculated by means of a Monte Carlo code: as can be seen the predicted effects are very large, in particular in the central region of the A spectrum, where experimental data are lacking.

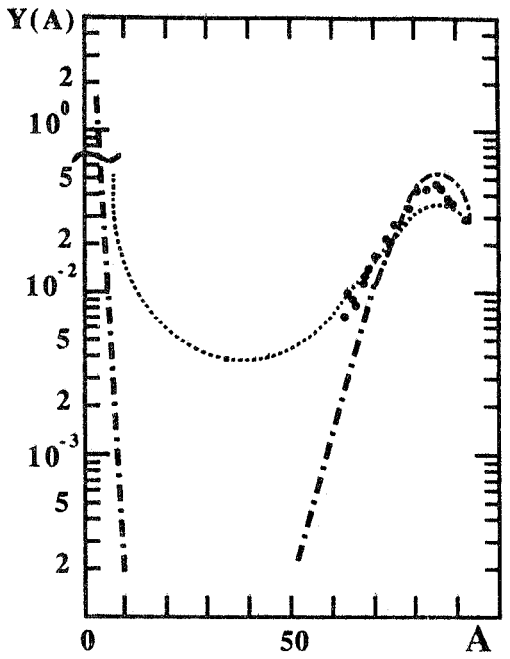

FIG.5 - Predicted mass distributions after annihilation of antiprotons on ^{95}Mo according to the Monte Carlo calculation of Ref.14: dash-dotted curve with only evaporation, dotted curve including multi-fragmentation of the thermalized residual nuclei. The full dots are the experimental results of Ref.18.

It is noteworthy to underline that studying the break up of a nucleus by antiprotons is much more then an alternative way compared to the most common tools, namely high energy proton-induced reactions and intermediate energy heavy ion reactions. Heavy ions gives rise, intrinsically, to a more complicated path. Furthermore, high energy protons and heavy ions are subject to another difficulty, namely the fact that impact parameters are mixed in the

observation. This is not the case for antiproton annihilation at rest, for instance, where the initial system is always "prepared" in the same way.

As shown in Fig. 6, photons of 1.1 GeV energy are able to produce rather similar nuclear excitation and similar compound nuclei as antiprotons annihilating at rest. Moreover, photons are, in this respect, very attractive, since, due to their electromagnetic interaction, they probe the whole target volume and are able to deposit in the core of the nucleus their energy with low angular momentum, so allowing to reach the required energy density (4-5 MeV excitation energy per nucleon). Hence, the new monochromatic photon beam from the Jet Target on Adone, with energy from 200 up to 1200 MeV, offers the opportunity for a clean experimental research of these effects.

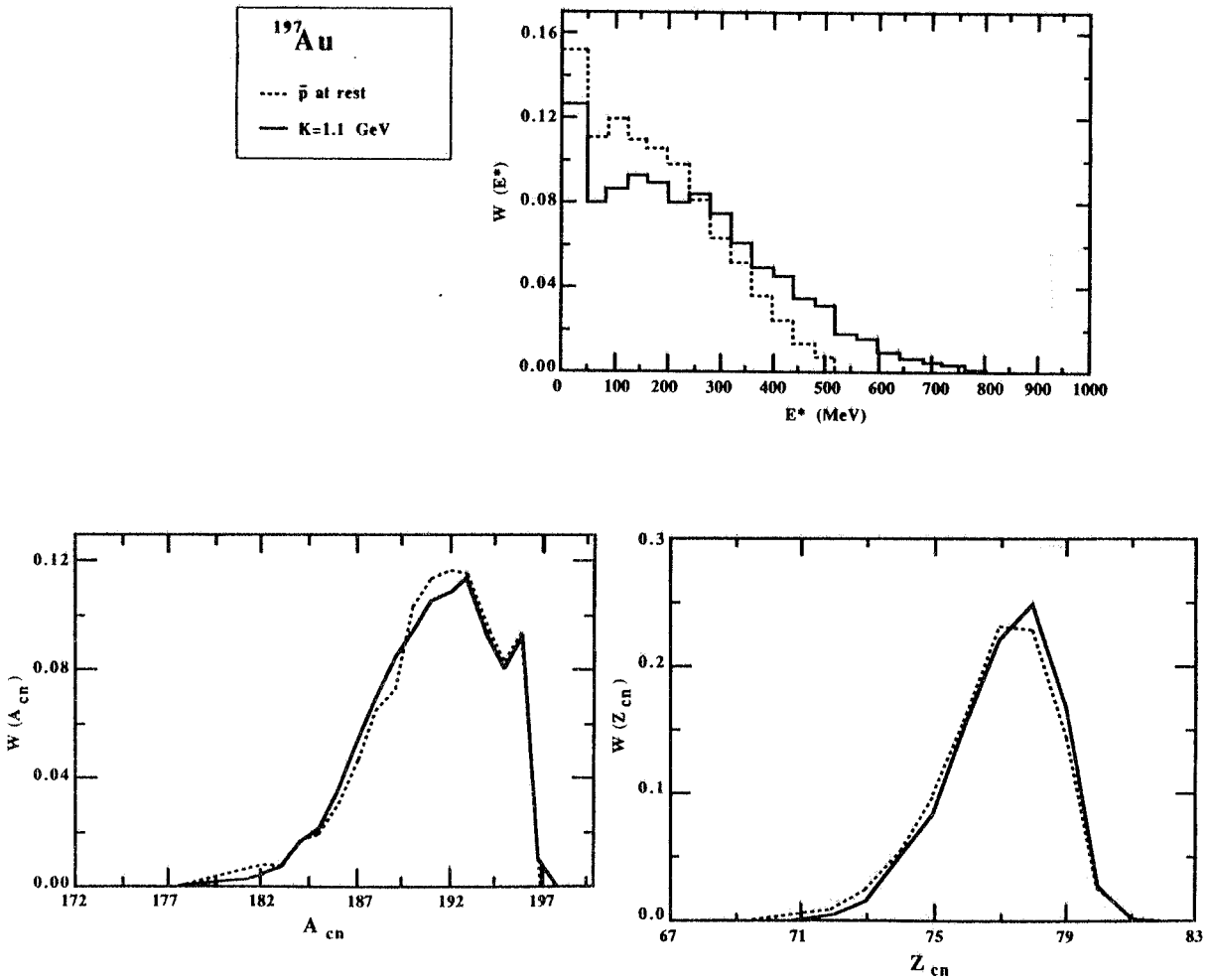

FIG.6 - Monte Carlo calculation of the distributions of excitation energy E* (a), mass A (b) and charge Z (c) of thermalized residual nuclei produced by low energy antiprotons and 1.1 GeV photons hitting ^{197}Au nuclei.

The theoretical predictions[15] for multifragmentation are rather explicit. In moderately hot nuclear systems ($3 \leq E^* \leq 5$ MeV/nucleon), "quasi-evaporation" (i.e. the break down into a large residual nucleus and one or two small fragments or nucleons) and "quasi-fission" (i.e. the break down into two fragments with approximately equal masses) can be observed

accompanying many-body break up of the hot nucleus into light fragments. At higher excitation energies (E*≥5 MeV/nucleon) the multifragmentation takes place and the mass spectrum decreases exponentially for light fragments with increasing A with less slope than a purely evaporation spectrum. This regime could be detected by studying the mass distributions of fission fragments and looking for deviation from the predictions of conventional fission theory, or looking directly to the mass yield distributions of fragments from the photonuclear event initiated by ≥ 1 GeV photons, which are very different for fission-like or multifragmentation-like decaying modes, as it is seen in Fig. 7 that shows the results of a combined INC and multifragmentation Monte Carlo calculation[19] of the expected spectra for 1 GeV photons hitting Au nuclei.

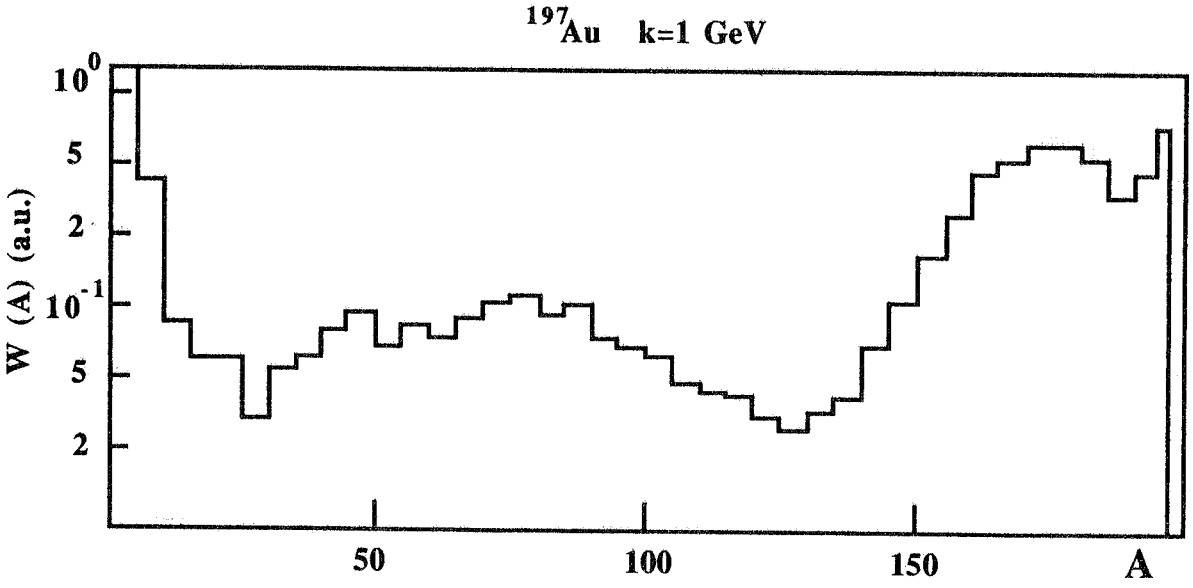

FIG.7 - The mass yield calculated by means of an intranuclear-multifragmentation-evaporation model, for the interaction of 1 GeV photons with ^{197}Au nuclei.

4. EXPERIMENTAL

4.1 The Jet Target Tagged photon beam

The photon beam is produced by bremsstrahlung of the electrons circulating in the ADONE storage ring of the Frascati Laboratories on an internal target consisting of a molecular Argon beam crossing, at supersonic speed, the ring vacuum pipe in the straight section N.5.[12] The target (Jet Target) is thin enough ($\approx 10^{-10}$ radiation length) that does not degrade the circulating beam quality, and allows several minutes of beam lifetime.

The Argon jet target system consists of three parts: i) the jet injection, where the jet is produced with the help of a special trumpet-shaped nozzle and several orifices; ii) the interaction

chamber, where the molecular jet crosses the electron beam at about 30 cm from its source point; iii) the jet dump, which ensures that the jet is pumped away without significant backstreaming. Three differential pumping stages have been interposed to separate both the jet-injection and the jet-dump chambers from the vacuum pipe in order to minimize the pressure rise in the interaction region. Each stage consists of a room between two successive orifices and is pumped on by a 360 l/s turbomolecular pump, which is directly flanged to the relevant vacuum chamber, while both the expansion and sink chambers are evacuated by a high speed (1000 l/s) turbomolecular pump. Two fast acting UHV valves separate the production and sink chambers from the ADONE vacuum pipe to easy the jet on/off operations and to prevent the possible contamination of the ring in case of a large pressure bump due to breakdown of the target system. The operating conditions are: inlet pressure and temperature 1÷20 bar and about 300 °K, respectively; nozzle throat diameter 70 μm and semiaperture 3.5°. From a total flux of $\approx 10^{20}$ Ar-atoms/s expanding from the nozzle, a collimator system selects about $10^{17} \div 10^{18}$ atoms/s, which correspond to a target thickness of 1÷10 ng/cm^2 (∅=6 mm) on the path of the electron beam. The operation of the target is controlled by a microprocessor-based system which performs all tasks to start up the jet on/off procedure, recording all the parameters, and safety checks.

The recoil electrons are momentum analyzed by the next ADONE bending magnet and detected by a two arrays of scintillation counters in coincidence (39 counters each array). This hodoscope is placed between the ring vacuum pipe and the magnet flux return joke. The scintillators define 76 energy channels and have different sizes in order to give a constant photon energy resolution (1%, for electrons of E_{e^-}=1500 MeV, and 2.7% for E_{e^-}=500 MeV) over the whole tagging range $\Delta k = (0.4 \div 0.8)\, E_{e^-}$. Each scintillator is connected to its phototube by means of optical fibers. The intensity of photons will be, under normal operating conditions (circulating electron current ≈60 mA and jet thickness 5 ng/cm^2), of $\approx 6\ 10^7$ photons/sec over the whole tagging range.

4.2 The fission chamber and detectors

The energy and mass distributions of the fission fragments will be measured using surface barrier silicon detectors, which have very good energy resolution (typically 50 KeV for the 5.48 MeV α-peak of the decay of ^{241}Am). These detectors have a very fast time response, suitable to use in conjunction with the tagging counters, which give the corresponding photon energy.

Initially, two detectors will be used, set at 180° from one another with the target in between: the optimal geometry to detect the two fission fragments in coincidence, due to their nearly isotropic distributions and the very low c.m. momentum. The detectors and the thin fission target will be put inside a vacuum chamber, so that fission fragments can be detected with minimum energy losses. The overall disposition is similar to that used in a previous experiment at lower energies with the LEALE monochromatic photon beam.[20]

The kinetic energies of the two correlated fragments will be obtained measuring the pulse height produced in the two facing detectors, after the calibration based on the measurements of the fission fragments in spontaneous fission of ^{252}Cf.[21]

To obtain the fragment masses M_1 and M_2 from their measured kinetic energies E_1 and E_2, respectively, an iteration procedure will be used to solve the following equations (obtained neglecting the momentum of the incoming photon):

$$M1 + M2 = A_f \tag{5}$$

$$M_1 = \frac{E_2 A_f}{E_1 + E_2} \tag{6}$$

where A_f is the mass of the fissioning nucleus. The A_f value must be selected taking into account the mean number of neutrons evaporated before fission. This is the principal main of this method: in this respect, however, two considerations can be done: a) the intranuclear-cascade plus evaporation Monte Carlo codes provides reliable values of A_f; b) the residual uncertainty in A_f does not influence greatly the obtained result, since an error of 4 A.M.U. in A_f is equivalent to an energy resolution of few %.

The two used detectors will have 600 mm^2 of area and will be put, inside the fission vacuum chamber, at 30 mm from the target, and at 90° with respect to the incoming photon beam direction. The target will be at 45° both with respect to the photon beam direction and to the line connecting the center of the two opposite detectors. Its thickness will be of 400 $\mu g/cm^2$, in order not to degrade the kinetic energy of the two emerging fragments.

The first nucleus studied will be ^{238}U, for which do not exist reliable data in the ≈1 GeV photon energy region since the mass distributions obtained with bremsstrahlung beams are dominated by the asymmetric behavior due to the Giant Resonance induced by the low energy photons of the spectrum.

In this conditions, considering an average cross section of 40 mb for U photofission in the tagged photon energy range of 600÷1200 MeV, and a photon flux in the same range of ≈6 10^7 photons/s, the expected counting rate is equal to ≈4 10^2 fissions/hour per detector (inclusive) over the whole tagged energy interval.

The coincidence (esclusive) counting rate is highly dependent on the geometry of the apparatus, due to the finite dimensions of the photon beam: in fact, in the same conditions as above, considering a gaussian spatial distribution of the photon beam with σ= 10 mm and center at the center of the target, the coincidence counting rate will be a factor 3 lower than the inclusive one. If the center of the photon beam is displaced of 2 mm from the center of the target, the coincidence efficiency will be lowered of a further 30%: so the beam-target alignment is very critical in this experiment. To allow for the correct the alignment of the photon beam on

the target, the vacuum chamber is equipped with two multiwire chambers[22] at the entrance and exit windows to monitor on-line the photon beam profile, while the same chamber is remotely controlled for up-down, left-right displacements, with a 0.1 mm precision, and turnable around the vertical axis with a 0.5 degree precision.

In Figure 8, a view of the fission chamber is given: Fig. 8a shows the disposition of target and detectors inside the vacuum chamber; Fig. 8b is a picture of the experimental apparatus installed in the experimental hall.

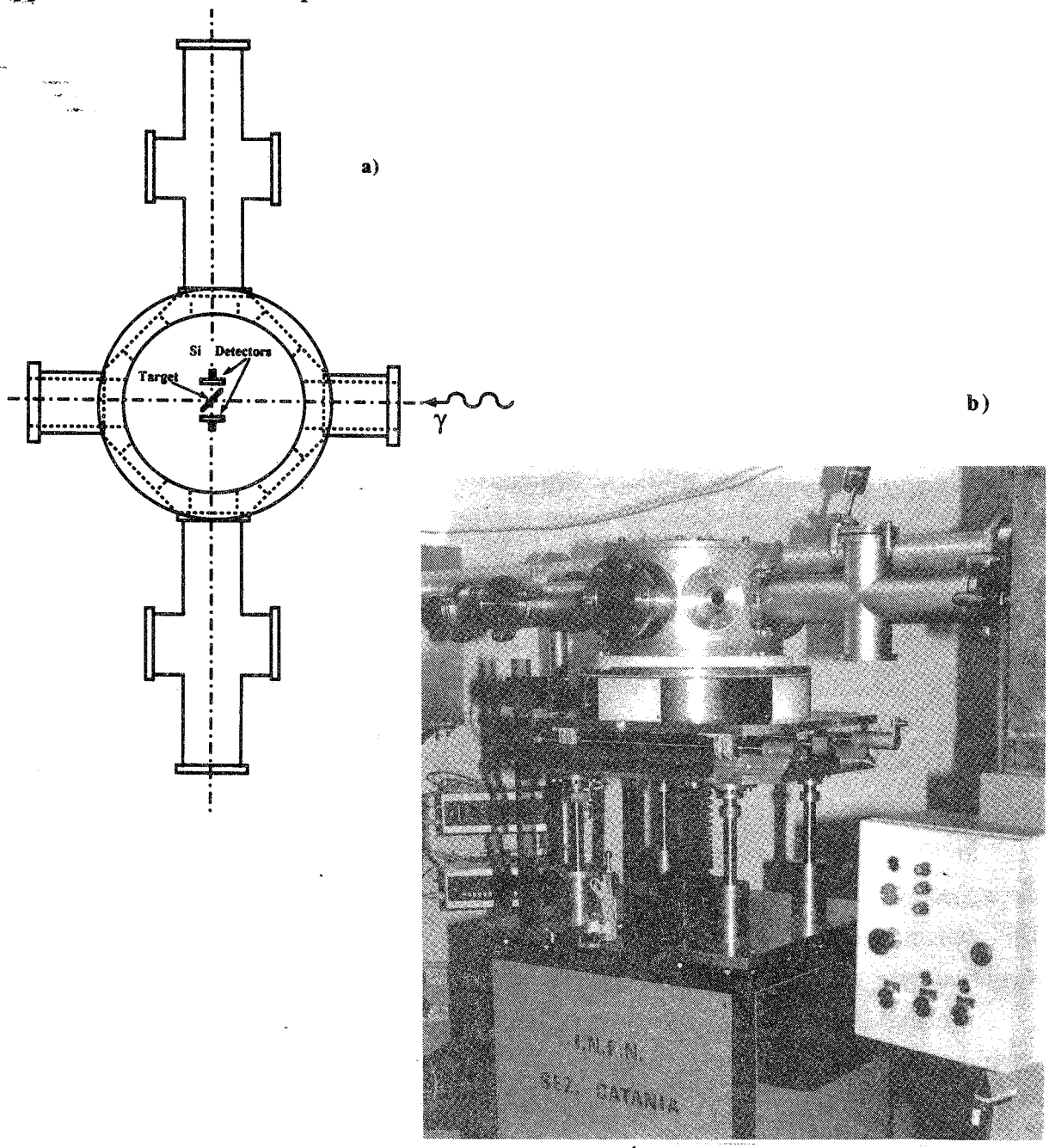

FIG. 8 - Schematic drawing of the fission vacuum chamber and fission fragments detectors (a); the fission chamber, with its support, mounted in the Jet Target experimental Hall (b).

Later, the experiment will be measure also the time and direction of flight of fission fragments to deduce the momentum $|\mathbf{P}|$ of the residual nucleus. To this end, the fission chamber is also arranged for the housing of detectors different from the silicon surface barrier ones, as PPAC, ionization chambers, wire chambers and scintillators, which also have very fast response suitable to be used in conjunction with the tagging counters. In particular, to make possible time-of-flight measurements, and hence to deduce directly the fragment mass distributions, the chamber is equipped, at both sides at 90 degree with respect to the photon beam direction, with two cylindrical arms of 40 cm each and diameter 10 cm, which provide a maximum basis of 55 cm for time-of-flight measurement with a solid angle of 30 msterad. In this way, measuring the kinetic energy E and the time T the fragment takes to travel the distance L, its mass will be simply given by:

$$M = \frac{2E\,T^2}{L^2} \tag{7}$$

and the distributions in energy and mass will be obtained without any assumption.

PPAC detectors used in transmission will provide the start signal for the time-of-flight measurement; they will be eventually modified for being position sensitive and giving information on the fragment emission angle, to determine its momentum. The stop signal will be provided by a system of silicon surface barrier detectors, which will also measure the fragment kinetic energy.

REFERENCES

1) A.S. Iljinov *et al.*, Sov. J. Nucl. Phys. **32**, 166 (1980).
2) J.P. Bondorf *et al.*, Phys. Lett. **162B**, 30 (1985).
3) V. Bellini *et al.*, Il Nuovo Cimento **85A**, 75 (1985).
   H. Ries *et al.*, Phys. Lett. **139B**, 254 (1984).
   J. Ahrens *et al.*, Phys. Lett. **146B**, 303 (1984).
4) H.A. Khan *et al.*, Phys. Rev. C **35**, 645 (1987).
   K.H. Hicks *et al.*, Phys. Rev. C **31**, 1323 (1985).
5) V.I. Noga *et al.*, Sov. J. Nucl. Phys. **43**, 856 (1986); **46**, 769 (1987).
6) J.P. Bocquet *et al.*, Phys. Lett. **182B**, 146 (1986); **192B**, 312 (1987).
7) L.N. Andronenko *et al.*, Z. Phys. **A318**, 97 (1984).
   F.D. Becchetti *et al.*, Phys. Rev. C **28**, 276 (1983).
8) V. Lucherini *et al.*, Phys. Rev. C **39**, 911 (1989).
   C. Guaraldo *et al.*, Phys. Rev. C **36**, 1027 (1987).
9) J.P. Bocquet *et al.*, *Physics at LEAR with low energy antiprotons*, ed. by C. Amsler *et al.* (Harward Acad. Publ., Chur, 1988), p.793.
   A. Angelopoulos *et al.*, Phys. Lett. 205B, 590 (1988).
   T.A. Armstrong *et al.*, Z. Phys. A331, 519 (1988).
   W. Markiel *et al.*, Nucl. Phys. A485, 445 (1988).
   T.A. Armstrong *et al.*, Z. Phys. A332, 467 (1989).
   S. Polikanov *et al.*, Nucl. Phys. **A502**, 195c (1989).
10) A.S. Iljinov *et al.*, Phys. Rev. C **39**, 1420 (1989).
11) C. Guaraldo *et al.*, Il Nuovo Cimento, in press [Frascati Preprint LNF-88/58(P)].
12) E. De Sanctis *et al.*, Few Body Suppl. 1, 414 (1986) and Frascati Report LNF-90/01(P).
13) E. Jones, in Physics at LEAR with Low-Energy Cooled Antiprotons, ed. by U. Gastaldi and R. Klapisch. E. Majorana Int. Scince Series, Vol.17, Plenum Press, New York and London, p.5 (1982).
14) A.S. Iljinov *et al.*, Nucl. Phys. **A382**, 378 (1982); Ye.S. Golubeva *et al.*, Nucl. Phys **A483**, 539 (1988).
15) A.S. Botvina *et al.*, Nucl. Phys. **A475**, 633 (1987)..
16) P. Fong, *Statistical Theory of Fission*, New York, Gordon and Beach 1969.
17) W.D. Myers and W.J. Swiatecki, Ark. Fys. **36**, 343 (1967).
18) E.F. Moser *et al.*, Phys. Lett. 179B, **25** (1986); E.F. Moser *et al.*, Z. Phys. **A333**, 89 (1989).
19) A.S. Botvina *et al.*, Phys. Lett. **205B**, 421 (1988) and Nucl. Phys., to be published.
20) S. Lo Nigro *et al.*, Il Nuovo Cimento **98A**, 643 (1987).
21) H. Schimtt *et al.*, Phys. Rev. B **137**, 837 (1965).
22) M. Albicocco *et al.*, N.I.M. **203**, 63 (1982).